Accepted version of article published in American Journal of Biological Anthropology, 2023, Volume 180, Issue 2, pp 370-385 https://doi.org/10.1002/ajpa.24679

Crown tissue proportions and enamel thickness distribution in early Pleistocene *Homo antecessor* maxillary premolars (Atapuerca, Spain).

Short title: Enamel thickness in *H. antecessor* premolars

Laura Martín-Francés[a,b,c,d,e1], María Martinón-Torres[c,f], Marina Martínez de Pinillos[c,g], Song Xing[c,h], Christophe Soligo[f], Cecilia García-Campos[c,i], Mario Modesto-Mata[c], José María Bermúdez de Castro[c,f].

a Centro Mixto Universidad Complutense de Madrid - Instituto de Salud Carlos III de Evolución y Comportamiento Humanos, 28029 Madrid, Spain
b Departamento de Paleontología, Facultad de Ciencias Geológicas, Universidad Complutense de Madrid, 28040, Madrid, Spain.
c CENIEH (National Research Center on Human Evolution), Paseo de la Sierra de Atapuerca 3, 09002 Burgos, Spain.
d Institut Català de Paleoecologia Humana i Evolució Social (IPHES), Zona Educacional 4, Campus Sescelades URV (Edifici W3), 43700 Tarragona, Spain.
e Universitat Rovira i Virgili, Departament d'Història i Història de l'Art, Avinguda de Catalunya 35, 43002 Tarragona, Spain
f Anthropology Department, UCL, 14 Taviton street, WC1H 0BW, London, United Kingdom.
g Laboratorio de Evolución Humana, Departamento de Historia, Geografía y Comunicación, Facultad de Humanidades y Educación, Universidad de Burgos, Plaza Misael Bañuelos s/n 09001 Burgos, Spain.
h Key Laboratory of Vertebrate Evolution and Human Origins of Chinese Academy of Sciences, Institute of Vertebrate Paleontology and Paleoanthropology, Chinese Academy of Sciences, Beijing 100044, China.
i Facultad de Ciencias Humanas y Sociales, Universidad Pontificia de Comillas, C/ Universidad Comillas, 3-5, 28049 Madrid, Spain.

1. Corresponding author: Laura Martín-Francés, Centro Mixto Universidad Complutense de Madrid - Instituto de Salud Carlos III de Evolución y Comportamiento Humanos, 28029 Madrid, Spain. lauramartinfrancesmf@gmail.com

Abstract

Objectives

Both morphometric and proteomic studies have revealed the close relationship of *Homo antecessor* with Neanderthals and *H. sapiens*. Considering this relationship, we aim to characterize the Early Pleistocene Atapuerca-Gran Dolina (TD6) maxillary premolars to test if their pattern of enamel thickness is shared with Neanderthals or *H. sapiens*.

Materials and Methods

We employed microcomputed tomography to estimate 2D and 3D tissue proportions in seven *H. antecessor* maxillary premolars, belonging to two individuals: H1 and H3, and compared them to a sample of extinct and extant *Homo* populations of African, Asian and European origin (n=52).

Results

Our results reveal a different pattern of enamel thickness between the Atapuerca-Gran Dolina two individuals. While TD6-H1 possesses thin-enameled crowns, with a clear affinity with

Neanderthals, TD6-H3 exhibits the thick pattern, a trait shared with the majority of fossil hominins and *H. sapiens*.

Discussion

This work provides new data on upper premolar enamel thickness in *H. antecessor*. By documenting both a thin and a thick pattern of enamel thickness in the TD6 sample, we warn about the taxonomic utility of this feature in the characterization of isolated remains. We suggest that the thin enamel condition would have emerged during the Early Pleistocene and it became the most frequent and typical condition in Neanderthals. Possible causes for the pattern observed in TD6 include sexual dimorphism or presence of two populations in the sample; however, population variability is the most plausible explanation with a character expression intermediate between those of Neanderthals and other members of the genus *Homo*. This interpretation is compatible with the phylogenetic position of *H. antecessor* close to the ancestor of Neanderthals and *H. sapiens*.

Keywords: permanent maxillary premolars, tissue proportions, enamel distribution, *Homo antecessor*, Atapuerca-Gran Dolina.

Introduction

The fossil collection of *H. antecessor* (Bermúdez de Castro et al., 1997) from Atapuerca-Gran Dolina (TD6) is one of the few hominin fossil assemblages representative of the European Early Pleistocene (Duval et al., 2018; Falguères et al., 1999; Parés et al., 2018) and thus, a critical part of the available evidence to explore the origin and evolution of the European Pleistocene populations. A series of morphometric studies revealed a unique mosaic of traits in *H. antecessor* (Arsuaga et al., 1999; Bermúdez de Castro et al., 1997; Bermúdez de Castro, Martinón-Torres, Arsuaga, & Carbonell, 2017; Gómez-Robles, Bermúdez de Castro, Martinón-Torres, & Prado-Simón, 2011; Gómez-Robles et al., 2007; Martinón-Torres et al., 2019). Especially, *H. antecessor* derived morphological features are, among others, related to the morphology of the face (Arsuaga et al., 1999), the pattern of facial bone remodelling during growth (Lacruz et al., 2013) and a modern-like pattern of dental development (Bermúdez de Castro et al., 2010; Bermúdez de Castro, Rosas, Carbonell, et al., 1999). While the majority of plesiomorphic traits were described in *H. antecessor* dentition, studies also identified derived features shared with Neanderthals (Gómez-Robles, de Castro, et al., 2011; Gómez-Robles et al., 2007; Martínez de Pinillos, Martinón-Torres, Martín-Francés, Arsuaga, & Bermúdez de Castro, 2017; Martinón-Torres et al., 2019). In addition, the characterization of the enamel thickness in the dental crowns of canines and molars evinced the combination of different patterns (García-Campos et al., 2019; Martín-Francés et al., 2018). That is, while the TD6 hominins possess relatively thick-enameled molars (Martín-Francés et al., 2018), the canines possess relatively thin enamel in their crowns (García-Campos et al., 2019), a condition shared with Neanderthals. To our knowledge, this is the only hominin population to present this combination of traits in its dentition.

Dental enamel is of interest to paleoanthropological studies regarding diet, growth, health and its potential to differentiate between species (Bayle et al., 2010; Dean et al., 2001; Macchiarelli et al., 2006; Martin, 1985; Olejniczak et al., 2008; Olejniczak et al., 2008; Smith et al., 2012; Smith, Toussaint, Reid, Olejniczak, & Hublin, 2007). The taxonomic value of enamel thickness is particularly diagnostic among European Neanderthals, as they are the only hominin species to present the thin condition, i.e., absolute and relatively thin enamel (Buti et al., 2017; Olejniczak et al., 2008; Smith et al., 2012). The mechanisms underlying the variations in dental tissue distribution is not clear and likely multifactorial. Several studies have hypothesised that the thin condition in Neanderthals can be related to odontogenetic mechanisms such as a faster developmental trajectory, a more complex topography and larger surface of the EDJ (Macchiarelli et al., 2006; Olejniczak et al., 2008; Smith et al., 2012; Suwa & Kono, 2005), whereas the thick condition in *H. sapiens* has been linked to unique odontogenetic processes and the extreme dental reduction (Grine, 2002; Grine, 2005; Smith et al., 2012).

Within the dentition, the characterization of enamel thickness in the molar series (M1-M3) identified a distinct trend of enamel increase in recent humans (Grine 2005) as well as in extinct species, including those from Atapuerca TD6 and SH (Smith et al., 2006; Martín-Francés et al., 2018, 202). This distalward increase was explained as the consequence of dental reduction (M1 > M2 > M3) that produces the loss of dentine in relation to the enamel. However, to our knowledge, there are no published data on the degree of enamel thickness variation in the premolar series.

The Early Pleistocene species, *H. antecessor* provides a unique opportunity to trace the origin of the thin enamel condition in the European hominin fossil record. By characterising the TD6 enamel thickness and its distribution, we test a. if the *H. antecessor* pattern of enamel thickness is shared with Neanderthals (thin condition) or with other hominins, including *H. sapiens*, (thick condition) and b. if *H. antecessor* shares the pattern of enamel thickness variation within the premolar series with Neanderthals and *H. sapiens*. For these purposes, we estimated 2D and 3D enamel thickness values and generate topographic thickness maps of the TD6 P^3s and P^4s (n=7) collection comparing them with those of extinct and extant hominin species (n=52). This study will also shed light on the taxonomic utility of enamel thickness.

Material

This study includes a total of 59 upper premolars (31 P^3s and 28 P^4s), including original and published data (Table 1). The TD6 premolar assemblage includes a total of seven premolars (four P^3s and three P^4s) belonging to two individuals. Specifically, Bermúdez de Castro et al., (2017a) assigned isolated specimens ATD6-7, ATD6-13 (P^3s) and ATD6-8 and ATD6-9 (P^4s) to individual H1 (TD6-H1), and ATD6-69 (right and left P^3s and right P^4 included in the maxillary bone) to individual H3 (TD6-H3). All TD6 specimens exhibit either wear category 1 (no wear) or 2 (minimal wear facets, no dentine exposure) based on Molnar's (1971) classification. In addition, and for comparative purposes, the study includes data of other 52 premolars belonging to extinct and extant populations of the genus *Homo* of African, Asian and European origin. We included original data of Neanderthals from La Quina and Krapina (n=8; available online on the NESPOS and ESRF databases, 2020), Chinese *H. erectus* from Zhoukoudian (n=2) and recent humans from Spain and China (n=24, 12 P^3s and 12 P^4s), as well as data extracted from the literature (n=18; Table 1). The Spanish dental assemblage used in this study derives from the forensic collection of the Anatomical Department of the Escuela de Medicina Legal y Forense (School of Legal and Forensic Medicine), Universidad Complutense de Madrid (UCM). The burials were recovered following the closure of two cemeteries located within the metropolitan area of Madrid, Spain. The Chinese samples come from the archaeological sites of Hubei and Henan (central China). According to the associated artefacts, these remains belong to an age range from Neolithic to Ming-Qing Dynasty. The Spanish and Chinese µCT data are stored at CENIEH (Burgos, Spain) and IVPP (Beijing, China), respectively.

Methods

Scanning of the samples

High-resolution µCT scanning of the fossil and recent material was performed in two laboratory facilities, the TD6 and recent human Spanish collections at CENIEH (Spain) and the Zhoukoudian and recent human Chinese collections at IVPP (China). The TD6 isolated premolars (ATD6-7, ATD6-13, ATD6-8 and ATD6-9) were scanned with a Scanco Medical Micro-CT80 system, using the following parameters: 70 kV and 114 mA, 0.1 Al filter and isometric voxel size of 18µm. With the acquisition of a new equipment at CENIEH in 2015, the three premolars included in the maxillary fragment ATD6-69 and the recent sample were scanned with a GE 103 Phoenix v/tome/x_s 240 instrument. Specimen ATD6-69 was scanned using the following parameters 120 kV, 120 µA, 0.2 mm Cu filter, and isometric voxel size of 0.67 mm. The recent human sample parameters were 100kV and 100µA, 0.2 Cu filter and voxel of 18µm. Moreover, the premolars of Zhoukoudian and Chinese recent humans were scanned using a 225kV-µCT scanner (designed by the Institute of High Energy Physics, Chinese Academy of Sciences, and housed at the Institute of Vertebrate Paleontology and Paleoanthropology, Chinese Academy of Sciences). The employed settings were 120kV, 100 µA, and voxel size of between 18.82 µm and 22.39 µm for the Zhoukoudian P^3 and P^4, respectively, and from 36.07 to 45.48 µm for recent humans.

Virtual segmentation

Measurements of 2D and 3D tissue proportions were collected by L MF and XS separately. Inter- and intra-observer error was assessed by three of the authors (L MF, M MP, and XS) performing the complete process, including orientation of the specimen, mesial plane definition, measures of the variables in each specimen. Each set of measurements was repeated in three alternate days, and the inter- and intra-observer error resulted in < 4%, thus not affecting the accuracy of the measurements (Zanolli et al., 2014 and therein).

2D virtual sectioning of the premolars was performed using Amira (6.3.0, FEI Inc.) and measured in ImageJ (1.51, NIH) following the protocol described in Feeney et al. (2010). The µCT image stack was imported into Amira (6.3.0, FEI Inc.) and oriented so the 3D model of each tooth was in occlusal view. In the corresponding 2D occlusal slice, the image stack was scrolled to the base of the crown. Then, the image stack was oriented to acquire a uniform ring of enamel. In this new orientation, the buccal and lingual dentine horns were located. The image stack was then readjusted with both dentine horns aligned horizontally. Finally, the image stack was centred at the buccal dentine horn and adjusted in mesiodistal rotation to pass through both dentine horns and between the maximal bicervical diameter and maximum cervical enamel extension (Feeney et al., 2010 and see Fig. 1 of this study). In the resulting 2D slice, we measured enamel (c) and coronal dentine (b, including the pulp) areas (in mm^2), total crown area (a, in mm^2), and enamel-dentine junction (EDJ) length (e, in mm) using ImageJ (1.51, NIH). Finally, we calculated the average enamel thickness (AET=c/e), the relative enamel thickness ($RET= 100*AET/(b^{1/2})$ and the percentage of dentine and pulp in the premolar crown (=b/a*100 in %) (Martin, 1983; Olejniczak et al., 2008).

3D virtual segmentation of the dental tissues (enamel, dentine and pulp) was performed in Amira (6.3.0, FEI Inc.). We used the semiautomatic tool, threshold-based segmentation. We employed Olejniczak et al. (2008) protocol for the definition of the cervical plane. That is, the plane is halfway between the most apical continuous ring of enamel and the plane containing the last hint of enamel. The following variables were measured and/or calculated: volume of enamel (Ve in mm^3); volume of coronal dentine including the pulp enclosed in the crown (Vcdp in mm^3); total volume of the crown, including the enamel, dentine and pulp (Vc in mm^3); surface of the EDJ (SEDJ in mm^2); 3D average enamel thickness (3D AET=Ve/SEDJ in mm); 3D relative enamel thickness ($3D\ RET=100*3D\ AET/(Vcdp^{1/3})$, a scale-free measurement), and percentage of dentine and pulp in the total crown volume (Vcdp/Vc =100*Vcdp/Vc in %) (Kono, 2004; Olejniczak et al., 2008).

Statistical analyses

Enamel thickness. Due to the small TD6 sample size, we performed adjusted Z-score, comparing individually each TD6 specimen against the Neanderthal and recent human groups. The Adjusted Z-score test (Maureille, Rougier, Houet, & Vandermeersch, 2001; Scolan, Santos, Tillier, Maurelli, & Quintard, 2012) allows the comparison of unbalanced and reduced samples (one specimen against a group) by using Student's inverse t distribution. Adjusted Z-scores of AET, RET and percentage of dentine variables were computed to compare 2D and 3D dental tissue proportions and enamel thickness values of the TD6 specimens to the means and standard deviations of the Neanderthal and RH groups. In these Z-scores the -1.0 to +1.0 interval comprises the 95% of the variation in the reference sample.

Metameric variation. To illustrate the degree of enamel thickness variation in the premolar series, we conducted the dummy regression of AET, RET and percentage of dentine values. Multivariate regressions of enamel thickness on dummy variables allow studying the correlation of enamel thickness with non-metric variables such as the premolar position (Hardy, 1993).

Polymorphism versus expected intrapopulation variability. In order to evaluate quantitatively whether RET values in TD6 might be indicative of polymorphism, we derived all possible pairwise distances between individual RET values in the recent human sample and compared the distribution of recent human values to the differences between RET values in the TD6 specimens. We repeated the same analysis with the Neanderthal sample to compare the distribution of Neanderthal pairwise distance values to the distances between RET values in the TD6 specimens. All pairwise differences were scaled by dividing them by the average of the two values in order to account for overall differences in RET between populations. Analogous to a 1-tailed hypothesis test with a probability threshold of $p=0.05$, a TD6 pairwise difference value that falls within or above the upper 5% tail of the total distribution of recent human or Neanderthal pairwise differences, could be considered evidence suggestive of more pronounced variability and, indirectly, polymorphism in TD6 compared to recent humans or Neanderthals. The test was conducted in R 4.0.3 (R Core Team, 2020).

Enamel thickness distribution

Using Amira (6.3.0, FEI Inc.) we generated chromatic maps to visualize the enamel thickness topographic distribution in the TD6 premolar crowns (P^3: ATD6-7 and right AT6-96; P^4: ATD6-8 and right ATD6-69) and compare them to those of a Neanderthal (La Quina P^3 and P^4) and recent humans of Spanish origin (P^3 and P^4). The defined chromatic scale is from thinnest (blue) to thickest (red) (Bayle, Le Luyer, & Robson Brown, 2017; Macchiarelli, Bayle, Bondioli, Mazurier, & Zanolli, 2013). For representation purposes, left premolars were mirror-imaged. In addition, to minimise the subjectivity in the interpretation of the chromatic maps, we assessed thickness variability in the 2D cross-sections. Following Grine (2005) we measured LTL: maximum linear enamel thickness on the lingual side of the lingual cusp, measured perpendicular to the EDJ at a point approximately 1 mm cervical to the dentine horn. CTL: linear enamel thickness on the apex of the lingual cusp, it is the distance between the apex of the dentine horn and the tip of the cusp. i: maximum linear thickness of occlusal enamel on the lingual cusp (protocone), measured perpendicular to the EDJ. h: Maximum linear thickness of occlusal enamel on the buccal cusp (paracone) measured perpendicular to the EDJ. CTB: Linear enamel thickness on the apex of the buccal cusp, it is the distance between the tip of the dentine horn and the tip of the cusp. LTB: Maximum linear enamel thickness on the buccal side of the buccal cusp, measured perpendicular to the EDJ at a point approximately 1 mm cervical to the dentine horn. Moreover, using the lingual and buccal linear measurements as markers, we measured the buccal (Bucc), lingual (Ling) and occlusal (Occl) areas defined as Bucc: area of the buccal surface from the cervix to the LTC. Ling: area of the lingual surface from the cervix to the CTB. Occl: Area of the occlusal basin between the LTC and the CTB (Fig. 2).

Results

Considering the TD6 (P^3s=4 and P^4s=3) 2D and 3D estimated mean values for AET, RET and percentage of dentine, the TD6 maxillary premolars exhibit intermediate values between those of the Neanderthals and fossil and recent *H. sapiens* (Tables 2 and 3; Figs. 3 and 4). However, considering the small sample size (total n=7) and the disparate results between the two individuals (H1 and H3), we decided to address the TD6 estimates individually (Tables 2 and 3) instead of considering the mean values.

2D enamel thickness. Estimates obtained from virtual cross-sections indicate that the P^3s (ATD6-7 and ATD6-13) and P^4s (ATD6-8 and ATD6-9) of TD6-H1 have relatively thin enamel compared to both fossil *H. sapiens* (Zanolli et al., 2019) and recent humans (this study). For the RET variable, TD6-H1 is outside the range of variation of this group (Table 2 Fig. 3) but within the Neanderthal variation range (Bayle et al., 2017; Zanolli et al., 2019 and this study). Relatively thin enamel in TD6-H1 is attributed to the greater percentage of dentine area; closer to the Neanderthal mean values than to fossil *H. sapiens* and recent humans mean values. Conversely, the ATD6-69 P^3s and P^4s of TD6-H3 have average and relatively thick enamel compared to Neanderthals, outside their range of variation, but within the range of variation of both fossil *H. sapiens* (Zanolli et al., 2019) and recent humans (this study). Thick AET and RET in TD6-H3 results from a combination of larger enamel area and shorter EDJ and the smaller dentine area per unit of crown area, similar to those of *H. sapiens* groups.

As for the rest of the comparative sample, TD6-H1 (P^3s: ATD6-7 and ATD6-13, and P^4s: ATD6-8 and ATD6-9) presents thin AET and RET and higher percentage of dentine compared to South African *Homo* (SAH), specimen SK27, the East African *Homo* (EAH) specimen KNM-ER 1590, Asian Early *Homo* (AEH) from Sangiran, specimen S7-4, North Africa *Homo* (NAH) from Thomas Quarry, and European *Homo* (EH) from Steinheim (Smith et al., 2012) (Table 2 and Fig. 3). TD6-H3 (ATD6-69 P^3s and P^4s) AET and RET values are close to those reported for NAH from Thomas Quarry (Smith et al., 2012) (Table 2 and Fig. 3).

3D enamel thickness. As described for the 2D variables, the TD6 individuals present contrasting results. While TD6-H1 is characterised by thin-enameled crowns, TD6-H3 presents thick-enameled crowns. That is, TD6-H1 premolars possess thin AET and RET with values close to those of Neanderthals (Zanolli et al., 2019, Bayle et al., 2017 and this study) and Asian early *Homo* (AEH) from Zhoukoudian (specimen PA67). For the RET variable, TD6-H1 premolars are outside the range of variation for both fossil *H. sapiens* and recent humans. Thinner enamel in TD6-H1 results from the greater dentine volume per unit crown volume (Table 3 and Fig. 4). Conversely, TD6-H3 premolars exhibit thick RET, close to the mean values of recent humans and outside the range of variation of Neanderthals. TD6-H3 thick enameled premolars result from the smaller dentine volume per unit of crown volume (Table 3 and Fig. 4).

Statistical Analysis. The statistical results reflect the described pattern for TD6-H1 and TD6-H3 for both 2D (Fig. 5) and 3D (Fig. 6) estimates. Although TD6 individuals fall within the 95% of variation of Neanderthals (NEA) and recent human (RH) for most of the variables, TD6-H1 closely resembles the Neanderthal condition while TD6-H3 resembles the thick *H. sapiens* condition (Figs. 5 and 6).

Despite the differences observed between TD6 individuals, the 2D and 3D estimates of the premolars are concordant. That is, TD6-H1 premolars have thinner enamel than recent humans and similar to Neanderthals in both 2D and 3D. Similarly, TD6-H3 premolars have thicker enamel than Neanderthals, similar to that of recent humans in both 2D and 3D estimates. Regarding the different pattern (thin versus thick) observed between the TD6 individuals, in TD6-H1 it can be attributed to the combination of larger dentine area and larger EDJ length in 2D results and larger dentine volume in 3D results, in comparison to TD6-H3 (Fig. 7). Moreover, as it was observed for molars (Olejniczak et al., 2008), in 2D cross-sections all species show greater proportion of dentine than in 3D (Fig. 7). However, the difference of dentine proportions between the 2D and 3D estimations across species in premolars is not as pronounced as it is in molars (Olejniczak et al., 2008). Thus, for premolars, it seems that 2D cross-sections are a good proxy for characterizing the whole-crown enamel thickness (Fig. 7).

Metameric variation. Figure 8 depicts the metameric variation in *H. antecessor,* Neanderthals and recent humans. Although we detected an increasing trend of AET and RET, as well as decrease of the dentine proportion from P^3 to P^4 in all groups, TD6 presents the least variation (lower degree of slope) for both 2D and 3D analysis and for the three variables.

Polymorphism versus expected intrapopulation variability. When comparing pairwise differences in RET values among Neanderthals and recent humans to the corresponding difference in RET values between the two TD6 individuals, 2 out 28 pairwise differences among Neanderthals were higher than the difference between the TD6 individuals for P^3 (7.1%), and 2 out of 15 pairwise differences among Neanderthals were higher than the difference between the TD6 individuals for P^4 (13.3%). Similarly, 10 out of 66 pairwise differences in recent humans were larger than the difference between the TD6 individuals for P^3 (15.2%), and 21 out of 66 pairwise differences in recent humans were larger than the difference between the TD6 individuals P^4 (31.8%). As such, the differences in RET values between TD6 individuals fell within the lower 95% of corresponding values derived from the Neanderthal and recent human samples for both P^3 (92.9% and 84.8%, respectively) and P^4 (86.7% and 68.2%, respectively).

Enamel thickness topographic distribution. The chromatic maps of enamel thickness distribution in TD6 and of the comparative sample (NEA=Neanderthals and RH= recent humans) are shown in Figs. 9 (P^3) and 10 (P^4). Overall, there are minimal differences among the investigated specimens (TD6, NEA and RH). Thicker enamel distributes over the buccal and lingual surfaces, especially in the protocone.

When comparing the relatively thicker ATD6-69 specimens belonging to TD6-H3 with those associated to TD6-H1 (ATD6-7 and ATD6-8), the distribution cartographies in ATD6-69 specimens reveal a wider concentration of enamel thickness in the occlusal basin. This characteristic is shared with RH specimens, especially for the P^4.

Additionally, following Grine (2005), we performed nine measurements in the 2D cross-sections (Fig. 2) to evaluate intra- and interspecies thickness variation (Table 4). Similarly to what we observed for the enamel thickness distribution (Figs. 5 and 6), there is a marked difference between TD6 individuals for the CTL and Occl variables. That is, TD6-H3 presents higher values of enamel thickness in the lingual (protocone) cusp (CTL) and in the occlusal basin compared to TD6-H1 (Table 4). Similarly, for these variables, the estimated values for TD6-H1 are within the Neanderthal variation range, but outside the recent human group; conversely, TD6-H3 is within the recent human range of variation but outside the Neanderthal variation range.

Overall, TD6-H3 exhibits higher values of enamel thickness compared to TD6-H1 and Neanderthals in both the occlusal and lingual cusp that correspond to the widespread red areas in the chromatic maps (Figs. 5 and 6).

Discussion

Our results show that some *H. antecessor* permanent upper premolars show a mixture of enamel thickness pattern, thin and thick, and a subtle metameric variation of enamel thickness compared to Neanderthal and recent human groups. This finding adds more complexity to the interpretation of the evolution of this trait as well as its taxonomic validity.

While TD6-H1 exhibits thin enameled premolar crowns, in common with Neanderthals, TD6-H3 exhibits the thick pattern in their crowns shared with the majority of fossil hominins and recent humans. Previous results on *H. antecessor* dentition concluded that TD6 molars are characterised by thick enamel (Martín-Francés et al., 2018) while the canines show the thin condition (García-Campos et al., 2019). Although previous analyses of Atapuerca dental remains, including TD6 and SH (García-Campos et al., 2019; Martín-Francés et al., 2020), already recorded a mixed pattern in the dentition (thick enameled molars and thin enameled canines), this is the first time that the combination of thin and thick patterns are recorded in the same dental class. Moreover, as the number of studies on enamel thickness increases (e.g., Zanolli et al., 2014; Martín-Francés et al., 2018, 2020; García-Campos et al., 2019; Martínez de Pinillos et al., 2020), results suggest that this trait may not be as taxonomically discriminative for the genus *Homo* as previously thought, with the exception, perhaps, of Neanderthals (Olejniczak et al., 2008; Smith et al., 2012; Buti et al., 2017; Zanolli et al., 2019).

Still, the underlying causes behind the pattern of hominin enamel thickness remains elusive. Not only is enamel formation a highly complex process involving proteins from at least six different genes (Hlusko, Suwa, Kono, & Mahaney, 2004; Robinson, Brookes, Shore, & Kirkham, 1998), but we also know that the genetic mechanisms that produce an organ are not necessarily the same ones that determine variation (Hlusko et al., 2004; Jernvall, 2000). Several hypotheses have been proposed to explain the different patterns of enamel thickness (thin versus thick) in hominins. Some of them include the reliance on tool use or food preparation that resulted in thinner enamel during the evolution of *Homo* (Teaford, 2007; Wrangham, Jones, Laden, Pilbeam, & Conklin-Brittain, 1999; but see Smith et al., 2012). Other scholars suggest specific odontogenetic mechanisms (Beynon & Wood, 1987; Dean et al., 2001; Macchiarelli et al., 2006; Smith et al., 2007) so the relatively thin enamel condition documented in Neanderthals could be linked to a faster developmental trajectory (Macchiarelli et al., 2006; Smith et al., 2007). Along the same line, investigations on *H. sapiens* relate their relatively thick enamel to a unique odontogenetic process different from that of *Australopithecus* and other species of the genus *Homo* (Dean et al., 2001). In this respect, Smith and colleagues (2012) suggested that the extreme dental reduction in *H. sapiens* was the cause of dentine reduction and, consequently, of the relatively thick enamel in this species.

This same mechanism (tooth reduction) was argued to explain the metameric increase expressed by enamel thickness along the molar row (Grine 2005; Smith et al., 2006). Distalward increase in enamel thickness was related to dental reduction which, in turn, produces a relative reduction of the dentine when compared to enamel. Consequently, absolute and relative enamel thickness increases (Grine 2005; Smith et al., 2006). Our results reflect that TD6 premolars are characterised by a subtle increasing pattern compared to Neanderthals and recent humans. That is, TD6 displays the lowest intra-species increase of metameric variation in enamel thickness along the premolar series. This effect could be mitigated in the case of TD6 due to the similar crown size of the P^3 and P^4 (H1-P^3 and P^4, MD=8.8 and 8.8 mm and BL 11.5 and 12.1 mm, respectively) which results in a similar percentage of dentine volume in P^3 and P^4s (Tables 2, 3 and Fig. 8). In contrast, for Neanderthals and recent humans, the marked increasing trend of enamel thickness from P^3 to P^4 reflects size reduction, specifically dentine reduction, of the P^4 with respect to the P^3.

We suggest at least four different causes for the combination of thin and thick enamel pattern recorded in TD6 H1 and H3. First, the pattern of enamel thickness could be linked to odontogenic factors. Researchers related the thin enamel of Neanderthals to a faster developmental trajectory (Smith et al., 2007; Macchiarelli et al., 2006) and the thick pattern in *H. sapiens* to a slow trajectory of enamel growth (Dean et al., 2001). In this regard, Bermúdez de Castro and collaborators (2010) estimated that the formation and eruption times in individual TD6-H5 was within the range of recent human populations and provided evidence of a shift in the pattern of dental development between *H. antecessor* and other early African and Asian hominins. However, a recent study concluded that lateral enamel in *H. antecessor* grew on average 27% faster than in *H. sapiens* (Modesto-Mata et al., 2020). More information on cuspal enamel and root formation times is required in order to give a more accurate estimation of the absolute timing of dental maturation in this species. Still, with the information available, it is not possible to relate the thick enamel on *H. antecessor* to a modern-like pattern of dental development, moreover this would only explain TD6-H3 values.

Second, we could explain the occurrence of the thin versus thick condition as consequence of sexual dimorphism. Studies concluded that females have thicker enamel compared to males (Smith et al., 2006; García-Campos et al., 2018; 2020; Sorenti et al., 2020). Based on the results obtained in this study, *H. antecessor* H1 could potentially represent a male and TD6-H3 a female. According to García-Campos et al., (2021) the differences observed between ATD6-13 and ATD6-69 are similar to those identified in recent humans between male and female dentitions (e.g.,Feeney et al., 2010; García-Campos, Martinón-Torres, Martín-

Francés, et al., 2018; García-Campos, Martinón-Torres, Martínez de Pinillos, et al., 2018; García-Campos et al., 2020; Saunders, Chan, Kahlon, Kluge, & FitzGerald, 2007; Sorenti, Martinón-Torres, Martín-Francés, & Perea-Pérez, 2019). However, these results would contrast with the analysis of enamel thickness in TD6 molars, where both H1 and H3 revealed a thick pattern (Martín-Francés et al., 2018). Therefore, it could be argued that the genetic signal linked to the expression of the enamel thickness pattern that characterizes females (thick enamel) or males (thin enamel) in *H. antecessor* is not as marked in molars as it is in canines. The pattern in *H. antecessor* would be different from that of recent humans where sexual dimorphism was also recorded in molars (Smith et al., 2006; Sorenti et al., 2019). These results highlight that more than one factor may be responsible for the variability of enamel thickness.

A third possibility is that TD6-H1 and H3 represent two different populations. TD6-H3 would represent a population where the enamel thickness trait preserves the condition expressed by early *Homo* populations and recent humans, whereas TD6-H1 would belong to a second population, where this trait has already derived to the condition that will become characteristic of Neanderthals. However, the stratigraphic data and the morphology of the hominin remains question this possibility. The remains belonging to TD6-H1 and H3 were recovered in the lithographic subunit TD6.2 from an excavated area of 6m^2 (Carbonell et al., 1999) suggesting a short event for the accumulation. Moreover, the morphological analysis of the human remains identified a general homogeneity characterizing one population (e.g., Arsuaga et al., 1999; Bermúdez de Castro et al., 1999; Martinón-Torres et al., 2019).

Finally, the discrepancy in enamel thickness exhibited by TD6-H1 and TD6-H3 could correspond to a polymorphism in *H. antecessor*. Most discrete dental traits are variable in expression. One trait may characterize a significant part of the group, but it is not necessarily expressed by all the group members (e.g., Bailey, 2002; Martinón-Torres et al., 2007; Martinón-Torres, Bermúdez de Castro, Gómez-Robles, Prado-Simón, & Arsuaga, 2012; Scott, 1980; Scott & Turner II, 1997). As an example, although Neanderthal P_4s manifest the higher frequency of well-developed continuous transverse crest, this feature is not present in all individuals (Bailey, 2002). Similarly, morphological analyses of the TD6 dental collection identified a series of traits that are variable in their frequencies (e.g., Martínez de Pinillos et al., 2017; Bermúdez de Castro et al., 2017; Gómez-Robles et al., 2011; Martinón-Torres et al., 2019). For instance, the continuous trigonid crest pattern on lower molars is typical of Neanderthals (due to the high frequency of expression in this species) and only partially represented in TD6 molars (ATD6-112 and ATD-113, Martínez de Pinillos et al., 2017). Similarly, GM analysis of the enamel occlusal conformation of the maxillary premolars showed that while ATD6-7 clustered with SH and Neanderthals, ATD6-69 grouped with *H. sapiens* (Gómez-Robles et al., 2011). In this sense, we could hypothesize that the thin and thick conditions of TD6-H1 and H3, respectively, could be due to the expression of a polymorphism in this species. However, based on the statistical analysis comparing the variability between TD6 individuals to the variability expressed in the Neanderthal and recent human samples, this hypothesis also remains unsatisfying. While the differences in RET values between the two individuals from TD6 were higher than the average of the corresponding values derived from the Neanderthal and recent human samples for both P^3 and P^4, the analysis did not provide statistical support to the hypothesis of higher variability in *H. antecessor* than Neanderthals and recent humans based on currently available data. Therefore, extensive fossil data will be needed to evaluate the possibility of polymorphism directly.

Conclusion

This work provides new evidence on the dental enamel thickness characterization of the Early Pleistocene species *H. antecessor* (Atapuerca-TD6). We recorded a contrasting pattern of enamel thickness variation within the TD6 population. While individual H1 (represented by specimens ATD6-7, ATD6-8, ATD6-9, ATD6-13) presents the thin enamel pattern shared with Neanderthals, individual H3 (ATD6-69 specimens) possess the thick pattern, shared with most hominin fossil and recent humans. The complexity of the interpretation of these results is due to the multifactorial nature of enamel thickness ontogeny and the small sample size. Future findings in the TD6 level might provide new dental remains to shed further light on this topic.

Acknowledgements

The authors acknowledge all members of the Atapuerca Research Team for their dedication and effort. Special thanks to those who excavate at Sima de los Huesos and the Conservation and Restoration Department at CENIEH, in particular to Pilar Fernández-Colón, for their assistance during the preparation and scanning of the material. This study received financial support from the Spanish Ministry of Science and Innovation Project PID2021-122355NB-C33 financed by MCIN/AEI/10.13039/501100011033/ FEDER, UE and the Consejería de Cultura y Turismo of the Junta de Castilla y León (Spain). We acknowledge The Leakey Foundation through the personal support of Gordon Getty (2013) and Dub Crook (2014-2022) to one of the authors (MM-T). LM-F has received support from the Spanish Ministry of Science and Innovation through the "María de Maeztu" excellence accreditation (CEX2019-000945-M) and currently from the project IJC2020-043979-I financed by the MCIN/AEI/10.13039/501100011033, and NextGenerationEU/PRTR. Part of this research was performed at the CENIEH-ICTS, scan of TD6 and *H. sapiens* specimens were performed by LM-F in the CENIEH Microscopy Laboratory, and with the collaboration of the CENIEH staff.

Data Availability statement

This study concerns the analysis of an original fossil human sample. The TD6 specimens are currently stored at the National Research Centre on Human Evolution (CENIEH), Burgos, Spain. In addition, the mCT scans of recent human populations are stored at CENIEH (Spain) and IVPP (China). The data that support the findings of this study are available from the authors upon request.

References

Arsuaga, J.-L., Martínez, I., Lorenzo, C., Gracia, A., Muñoz, A., Alonso, O., & Gallego, J. (1999). The human cranial remains from Gran Dolina Lower Pleistocene site (Sierra de Atapuerca, Spain). *Journal of Human Evolution, 37*(3-4), 431-457. doi:http://dx.doi.org/10.1006/jhev.1999.0309

Bailey, S. E. (2002). A closer look at Neanderthal postcanine dental morphology: The mandibular dentition. *The Anatomical Record, 269*(3), 148-156. doi:https://doi.org/10.1002/ar.10116

Bayle, P., Macchiarelli, R., Trinkaus, E., Duarte, C., Mazurier, A., & Zilhão, J. (2010). Dental maturational sequence and dental tissue proportions in the early Upper Paleolithic child from Abrigo do Lagar Velho, Portugal. *Proceedings of the National Academy of Sciences, 107*(4), 1338-1342. doi:10.1073/pnas.0914202107

Bayle, P., Le Luyer, M., & Robson Brown, K.A. (2017). The Palomas dental remains: enemal thickness and tissues proportions. In E. Trinkaus & M. J. Walker (Eds.), *The people of Palomas: neandertals from the Sima de las Palomas del Cabezo Gordo, Southeastern Spain* (pp. 115–137). College Station, Texas.: A&M University Anthropology Series.

Bermúdez de Castro, J. M., Arsuaga, J. L., Carbonell, E., Rosas, A., Martínez, I., & Mosquera, M. (1997). A Hominid from the Lower Pleistocene of Atapuerca, Spain: Possible Ancestor to Neandertals and Modern Humans. *Science, 276*(5317), 1392-1395. doi:10.1126/science.276.5317.1392

Bermúdez de Castro, J. M., Carretero, J. M., García-González, R., Rodríguez-García, L., Martinón-Torres, M., Rosell, J., . . . Carbonell, E. (2012). Early pleistocene human humeri from the gran dolina-TD6 site (sierra de atapuerca, spain). *American Journal of Physical Anthropology, 147*(4), 604-617. doi:10.1002/ajpa.22020

Bermúdez de Castro, J. M., Martinón-Torres, M., Arsuaga, J. L., & Carbonell, E. (2017). Twentieth anniversary of *Homo antecessor* (1997-2017): a review. *Evolutionary Anthropology: Issues, News, and Reviews, 26*(4), 157-171. doi:10.1002/evan.21540

Bermúdez de Castro, J. M., Martinón-Torres, M., Martín-Francés, L., Modesto-Mata, M., Martínez de Pinillos, M., García, C., & Carbonell, E. (2017). *Homo antecessor:* The state of the art eighteen years later. *Quaternary International, 433*, 22-31. doi:http://dx.doi.org/10.1016/j.quaint.2015.03.049

Bermúdez de Castro, J. M., Martinón-Torres, M., Prado, L., Gómez-Robles, A., Rosell, J., López-Polín, L., . . . Carbonell, E. (2010). New immature hominin fossil from European Lower Pleistocene shows the earliest evidence of a modern human dental development pattern. *Proceedings of the National Academy of Sciences, 107*(26), 11739-11744. doi:10.1073/pnas.1006772107

Bermúdez de Castro, J. M., Martinón-Torres, M., Rosell, J., Blasco, R., Arsuaga, J. L., & Carbonell, E. (2016). Continuity versus discontinuity of the human settlement of Europe between the late Early Pleistocene and the early Middle Pleistocene. The mandibular evidence. *Quaternary Science Reviews, 153*(Supplement C), 51-62. doi:https://doi.org/10.1016/j.quascirev.2016.10.010

Bermúdez de Castro, J. M., Rosas, A., Carbonell, E., Nicolás, M. E., Rodríguez, J., & Arsuaga, J. L. (1999). A modern human pattern of dental development in Lower Pleistocene hominids from Atapuerca-TD6 (Spain). *Proceedings of the National Academy of Sciences of the United States of America, 96*(7), 4210-4213.

Bermúdez de Castro, J. M., Rosas, A., & Nicolás, M. E. (1999). Dental remains from Atapuerca-TD6 (Gran Dolina site, Burgos, Spain). *Journal of Human Evolution, 37*(3-4), 523-566. doi:http://dx.doi.org/10.1006/jhev.1999.0323

Beynon, A. D., & Wood, B. A. (1987). Patterns and rates of enamel growth in the molar teeth of early hominids. *Nature, 326*(6112), 493–496.

Buti, L., Le Cabec, A., Panetta, D., Tripodi, M., Salvadori, P. A., Hublin, J.-J., . . . Benazzi, S. (2017). 3D enamel thickness in Neandertal and modern human permanent canines. *Journal of Human Evolution, 113*, 162-172. doi:10.1016/j.jhevol.2017.08.009

Dean, C., Leakey, M. G., Reid, D., Schrenk, F., Schwartz, G. T., Stringer, C., & Walker, A. (2001). Growth processes in teeth distinguish modern humans from Homo erectus and earlier hominins. *Nature, 414*(6864), 628–631

Duval, M., Grün, R., Parés, J. M., Martín-Francés, L., Campaña, I., Rosell, J., . . . Bermúdez de Castro, J. M. (2018). The first direct ESR dating of a hominin tooth from Atapuerca Gran Dolina TD-6 (Spain) supports the antiquity of Homo antecessor. *Quaternary Geochronology, 47*, 120-137. doi:https://doi.org/10.1016/j.quageo.2018.05.001

Falguères, C., Bahain, J.-J., Yokoyama, Y., Arsuaga, J. L., Bermudez de Castro, J. M., Carbonell, E., . . . Dolo, J.-M. (1999). Earliest humans in Europe: the age of TD6 Gran Dolina, Atapuerca, Spain. *Journal of Human Evolution, 37*(3-4), 343-352

Feeney, R. N. M., Zermeno, J. P., Reid, D. J., Nakashima, S., Sano, H., Bahar, A., . . . Smith, T. M. (2010). Enamel thickness in Asian human canines and premolars. *Anthropological Science, 118*(3), 191-198.

García-Campos, C., Martinón-Torres, M., Martín-Francés, L., Martínez de Pinillos, M., Modesto-Mata, M., Perea-Pérez, B., . . . Bermúdez de Castro, J. M. (2018). Contribution of dental tissues to sex determination in modern human populations. *American Journal of Physical Anthropology, 166*(2), 459-472. doi:10.1002/ajpa.23447

García-Campos, C., Modesto-Mata, M., Martinón-Torres, M., Martín-Francés, L., Martínez de Pinillos, M., Arsuaga, J. L., & Bermúdez de Castro, J. M. (2019). Enamel and dentine dimensions of the Pleistocene hominins from Atapuerca (Burgos, Spain): A comparative study of canine teeth. C R Palevol 18: 72-89.

García-Campos, C., Modesto-Mata, M., Martinón-Torres, M., Martínez de Pinillos, M., Martín-Francés, L., Arsuaga, J. L., & Bermúdez de Castro, J. M. (2020). Sexual dimorphism of the enamel and dentine dimensions of the permanent canines of the Middle Pleistocene hominins from Sima de los Huesos (Burgos, Spain). *Journal of Human Evolution, 144*, 102793. doi:https://doi.org/10.1016/j.jhevol.2020.102793

Gómez-Robles, A., Bermúdez de Castro, J. M., Martinón-Torres, M., Prado-Simón, L., & Arsuaga, J. L. (2015). A geometric morphometric analysis of hominin lower molars: Evolutionary implications and overview of postcanine dental variation. *Journal of Human Evolution, 82*, 34-50. doi:http://dx.doi.org/10.1016/j.jhevol.2015.02.013

Gómez-Robles, A., de Castro, J. M. B., Martinón-Torres, M., & Prado-Simón, L. (2011). Crown size and cusp proportions in Homo antecessor upper first molars. A comment on Quam et al. 2009. *Journal of Anatomy, 218*(2), 258-262. doi:10.1111/j.1469-7580.2010.01324.x

Gómez-Robles, A., Martinón-Torres, M., Bermúdez de Castro, J. M., Margvelashvili, A., Bastir, M., Arsuaga, J. L., . . . Martínez, L. M. (2007). A geometric morphometric analysis of hominin upper first molar shape. *Journal of Human Evolution, 53*(3), 272-285. doi:http://dx.doi.org/10.1016/j.jhevol.2007.02.002

Gómez-Robles, A., Martinón-Torres, M., Bermúdez de Castro, J. M., Prado-Simón, L., & Arsuaga, J. L. (2011). A geometric morphometric analysis of hominin upper premolars. Shape variation and morphological integration. *Journal of Human Evolution, 61*(6), 688-702. doi:http://dx.doi.org/10.1016/j.jhevol.2011.09.004

Grine, F. E. (2002). Scaling of tooth enamel thickness, and molar crown size reduction in modern humans. *South African Journal of Science, 98*, 503-509.

Grine, F. E. (2005). Enamel thickness of deciduous and permanent molars in modern *Homo sapiens*. *American Journal of Physical Anthropology, 126*(1), 14-31. doi:10.1002/ajpa.10277

Hardy, M. A. (1993). *Regression with Dummy Variables*. Thousand Oaks, United States: SAGE Publications Inc.

Hlusko, L. J., Suwa, G., Kono, R. T., & Mahaney, M. C. (2004). Genetics and the evolution of primate enamel thickness: A baboon model. *American Journal of Physical Anthropology, 124*(3), 223-233. doi:10.1002/ajpa.10353

Jernvall, J. (2000). Linking development with generation of novelty in mammalian teeth. *Proceedings of the National Academy of Sciences of the United States of America, 97*(6), 2641-2645.

Kono, R. T. (2004). Molar enamel thickness and distribution patterns in extant great apes and humans: new insights based on a 3-dimensional whole crown perspective. *Anthropological Science, 112*(2), 121-146.

Lacruz, R. S., Bermúdez de Castro, J. M., Martinón-Torres, M., O'Higgins, P., Paine, M. L., Carbonell, E., . . . Bromage, T. G. (2013). Facial Morphogenesis of the Earliest Europeans. *PLoS ONE, 8*(6), e65199. doi:10.1371/journal.pone.0065199

Macchiarelli, R., Bayle, P., Bondioli, L., Mazurier, A., & Zanolli, C. (2013). From outer to inner structural morphology in dental anthropology: integration of the third dimension in the visualization and quatitative analysis of fossil remains. In G. R. Scott & J. D. Irish (Eds.), *Anthropological Perspectives on Tooth Morphology. Genetics, Evolution, Variation* (pp. 250-277). Cambridge: Cambridge Iniversity Press.

Macchiarelli, R., Bondioli, L., Debenath, A., Mazurier, A., Tournepiche, J.-F., Birch, W., & Dean, M. C. (2006). How Neanderthal molar teeth grew. *Nature, 444*(7120), 748-751. doi:10.1038/nature05314

Martín-Francés, L., Martinón-Torres, M., Martínez de Pinillos, M., García-Campos, C., Modesto-Mata, M., Zanolli, C., . . . Bermúdez de Castro, J. M. (2018). Tooth crown tissue proportions and enamel thickness in Early Pleistocene Homo antecessor molars (Atapuerca, Spain). *PLoS ONE, 13*(10), e0203334. doi:10.1371/journal.pone.0203334

Martín-Francés, L., Martinón-Torres, M., Martínez de Pinillos, M., García-Campos, C., Zanolli, C., Bayle, P., . . . Bermúdez de Castro, J. M. (2020). Crown tissue proportions and enamel thickness distribution in the Middle Pleistocene hominin molars from Sima de los Huesos (SH) population (Atapuerca, Spain). PLoS ONE, 15(6), e0233281. doi:10.1371/journal.pone.0233281

Martin, L. (1985). Significance of enamel thickness in hominoid evolution. *Nature, 314*(6008), 260-263. doi:10.1038/314260a0

Martin, L. B. (1983). *The relationships of the late Miocene hominoidea.* (Doctor of Philosophy), University College of London, London.

Martínez de Pinillos, M., Martinón-Torres, M., Martín-Francés, L., Arsuaga, J. L., & Bermúdez de Castro, J. M. (2017). Comparative analysis of the trigonid crests patterns in Homo antecessor molars at the enamel and dentine surfaces. *Quaternary International, 433*, 189-198. doi:http://dx.doi.org/10.1016/j.quaint.2015.08.050

Martinón-Torres, M., Bastir, M., Bermúdez de Castro, J. M., Gómez, A., Sarmiento, S., Muela, A., & Arsuaga, J. L. (2006). Hominin lower second premolar morphology: evolutionary inferences through geometric morphometric analysis. *Journal of Human Evolution, 50*(5), 523-533. doi:http://dx.doi.org/10.1016/j.jhevol.2005.12.004

Martinón-Torres, M., Bermúdez de Castro, J. M., Gómez-Robles, A., Arsuaga, J. L., Carbonell, E., Lordkipanidze, D., . . . Margvelashvili, A. (2007). Dental evidence on the hominin dispersals during the Pleistocene. *Proceedings of the National Academy of Sciences, 104*(33), 13279-13282. doi:10.1073/pnas.0706152104

Martinón-Torres, M., Bermúdez de Castro, J. M., Gómez-Robles, A., Bastir, M., Sarmiento, S., Muela, A., & Arsuaga, J. L. (2007). Gran Dolina-TD6 and Sima de los Huesos dental samples: Preliminary approach to some dental characters of interest for phylogenetic studies. In S. E. Bailey & J. J. Hublin (Eds.), *Dental Perspectives on Human Evolution.* (pp. 65-79). Dordrecht, The Netherlands.: Springer.

Martinón-Torres, M., Bermúdez de Castro, J. M., Gómez-Robles, A., Margvelashvili, A., Prado, L., Lordkipanidze, D., & Vekua, A. (2008). Dental remains from Dmanisi (Republic of Georgia): Morphological analysis and comparative study. *Journal of Human Evolution, 55*(2), 249-273. doi:doi: DOI: 10.1016/j.jhevol.2007.12.008

Martinón-Torres, M., Bermúdez de Castro, J. M., Gómez-Robles, A., Prado-Simón, L., & Arsuaga, J. L. (2012). Morphological description and comparison of the dental remains from Atapuerca-Sima de los Huesos site (Spain). *Journal of Human Evolution, 62*(1), 7-58. doi:http://dx.doi.org/10.1016/j.jhevol.2011.08.007

Martinón-Torres, M., Bermúdez de Castro, J. M., Martínez de Pinillos, M., Modesto-Mata, M., Xing, S., Martín-Francés, L., . . . Liu, W. (2019). New permanent teeth from Gran Dolina-TD6 (Sierra de Atapuerca). The bearing of Homo antecessor on the evolutionary scenario of Early and Middle Pleistocene Europe. *Journal of Human Evolution, 127*, 93-117. doi:https://doi.org/10.1016/j.jhevol.2018.12.001

Maureille, B., Rougier, H., Houet, F., & Vandermeersch, V. (2001). Les dents inférieures du Néandertalien Regourdou 1 (site de Regourdou, commune de Montignac, Dordogne): analyses métriques et comparatives. *Paleo 13*, 183–200.

Modesto-Mata, M., Dean, M. C., Lacruz, R. S., Bromage, T. G., García-Campos, C., Martínez de Pinillos, M., . . . Bermúdez de Castro, J. M. (2020). Short and long period growth markers of enamel formation distinguish European Pleistocene hominins. *Scientific Reports, 10*(1), 4665. doi:10.1038/s41598-020-61659-y

Molnar, S. (1971). Human tooth wear, tooth function and cultural variability. *American Journal of Physical Anthropology, 34*(2), 175-189. doi:10.1002/ajpa.1330340204

Olejniczak, A. J., Smith, T. M., Feeney, R. N. M., Macchiarelli, R., Mazurier, A., Bondioli, L., . . . Hublin, J.-J. (2008). Dental tissue proportions and enamel thickness in Neandertal and modern human molars. *Journal of Human Evolution, 55*(1), 12-23. doi:doi: DOI: 10.1016/j.jhevol.2007.11.004

Olejniczak, A. J., Smith, T. M., Skinner, M. M., Grine, F. E., Feeney, R. N. M., Thackeray, J. F., & Hublin, J. J. (2008). Three-dimensional molar enamel distribution and thickness in Australopithecus and Paranthropus. *Biology Letters, 4*(4), 406-410. doi:10.1098/rsbl.2008.0223

Parés, J. M., Álvarez, C., Sier, M., Moreno, D., Duval, M., Woodhead, J. D., . . . Carbonell, E. (2018). Chronology of the cave interior sediments at Gran Dolina archaeological site, Atapuerca (Spain). *Quaternary Science Reviews, 186*, 1-16. doi:https://doi.org/10.1016/j.quascirev.2018.02.004

R Core Team (2020). R: A language and environment for statistical computing. R Foundation for Statistical Computing, Vienna, Austria. URL https://www.R-project.org/.

Robinson, C., Brookes, S. J., Shore, R. C., & Kirkham, J. (1998). The developing enamel matrix: nature and function. *European Journal of Oral Sciences, 106 Suppl 1*, 282-291. doi:10.1111/j.1600-0722.1998.tb02188.x

Saunders, S. R., Chan, A. H. W., Kahlon, B., Kluge, H. F., & FitzGerald, C. M. (2007). Sexual dimorphism of the dental tissues in human permanent mandibular canines and third premolars. *American Journal of Physical Anthropology, 133*(1), 735-740. doi:doi:10.1002/ajpa.20553

Scolan, H. F., Santos, Tillier, A. M., Maurelli, B., & Quintard, A. (2012). à Las Pélénos (Monsempron-Libos, Lot-et-Garonne, France). *Paléo, Bulletins et mémoires de la Société d'anthropologie de Paris*, 24.

Scott, G. (1980). Population Variation of Carabelli's Trait. *Human Biology, 52*, 63-78.

Scott, G. R., & Turner II, C. G. (1997). *The Anthropology of Modern Human Teeth. Dental Morphology and its Variation in Recent Human Populations.* . Cambridge: Cambridge University Press.

Smith, T. M., Olejniczak, A. J., Tafforeau, P., Reid, D. J., Grine, F. E., & Hublin, J.-J. (2006). Molar crown thickness, volume, and development in South African Middle Stone Age humans. *South African Journal of Science, 102*(11-12), 513-517.

Smith, T. M., Olejniczak, A. J., Zermeno, J. P., Tafforeau, P., Skinner, M. M., Hoffmann, A., . . . Hublin, J.-J. (2012). Variation in enamel thickness within the genus Homo. *Journal of Human Evolution*(62), 395-411. doi:10.1016/j.jhevol.2011.12.004

Smith, T. M., Toussaint, M., Reid, D. J., Olejniczak, A. J., & Hublin, J.-J. (2007). Rapid Dental Development in a Middle Paleolithic Belgian Neanderthal. *Proceedings of the National Academy of Sciences of the United States of America, 104*(51), 20220-20225 %U http://www.pnas.org/content/20104/20251/20220.

Sorenti, M., Martinón-Torres, M., Martín-Francés, L., & Perea-Pérez, B. (2019). Sexual dimorphism of dental tissues in modern human mandibular molars. *American Journal of Physical Anthropology, 169*(2), 332-340. doi:10.1002/ajpa.23822

Suwa, G., & Kono, R. T. (2005). A micro-CT based study of linear enamel thickness in the mesial cusp section of human molars: reevaluation of methodology and assessment of within-tooth, serial, and individual variation. *Anthropological Science, 113*(3), 273-289.

Teaford, M. F. (2007). What do we know and not know about diet and enamel structure? . In P. S. Ungar (Ed.), *Evolution of the Human Diet* (pp. 56-76). Oxford: Oxford University Press.

Welker, F., Ramos-Madrigal, J., Gutenbrunner, P., Mackie, M., Tiwary, S., Rakownikow Jersie-Christensen, R., . . . Cappellini, E. (2020). The dental proteome of Homo antecessor. *Nature, 580*(7802), 235-238. doi:10.1038/s41586-020-2153-8

Wrangham, Richard W., Jones, James H., Laden, G., Pilbeam, D., & Conklin-Brittain, N. (1999). The Raw and the Stolen: Cooking and the Ecology of Human Origins. *Current Anthropology, 40*(5), 567-594. doi:10.1086/300083

Zanolli, C., Biglari, F., Mashkour, M., Abdi, K., Monchot, H., Debue, K., . . . Macchiarelli, R. (2019). A Neanderthal from the Central Western Zagros, Iran. Structural reassessment of the Wezmeh 1 maxillary premolar. *Journal of Human Evolution, 135*, 102643. doi:https://doi.org/10.1016/j.jhevol.2019.102643

Zanolli, C., Bondioli, L., Coppa, A., Dean, C. M., Bayle, P., Candilio, F., . . . Macchiarelli, R. (2014). The late Early Pleistocene human dental remains from Uadi Aalad and Mulhuli-Amo (Buia), Eritrean Danakil: Macromorphology and microstructure. *Journal of Human Evolution, 74*(0), 96-113. doi:http://dx.doi.org/10.1016/j.jhevol.2014.04.005

Table 1. Fossil and Recent samples used for crown 2D and 3D measurements.

Samples	**N**	**Tooth class**	**Specimens**	**References**
H. antecessor (TD6)	4	P^3	Atapuerca-Gran Dolina: ATD6-7, ATD6-8, ATD6-69_R and ATD6-69_L	Original data
East African early *Homo* (EAH)	1		KNM-ER- 1590	Smith et al., 2012
South African early *Homo* (SAH)	1		SK27	Smith et al., 2012
Asian early *Homo* (AEH)	2		S7-4 PA67	Smith et al., 2012 Original data
North African early *Homo* (NAH)	1		Thomas Quarry 3	Smith et al., 2012
Neanderthal (NEA)	8		Wezmeh 1 Las Palomas: SP 53, SP 60, SP 68 La Quina H18 Krapina: KRD39, KRD53, KRD112	Zanolli et al., 2019 Bayle et al., 2017 Original data from ESRF website Original data from NESPOS website
Fossil *Homo sapiens* (FHS)	2		Qafzeh 10, 15	Zanolli et al., 2019
Recent humans (RH)	12		Recent humans from China (n=6) Recent humans from Spain (n=6)	Original data
H. antecessor (TD6)	3	P^4	Atapuerca-Gran Dolina: ATD6-8, ATD6-9, ATD6-69	Original data
East African early *Homo* (EAH)	1		KNM-ER- 1590	Smith et al., 2012
Asian early *Homo* (AEH)	2		S7-4 PA68	Smith et al., 2012 Original data
North African *Homo* (NAH)	1		Thomas Quarry 3	Smith et al., 2012
European *Homo* (EH)	1		Steinheim	Smith et al., 2012
Neanderthal (NEA)	6		Las Palomas: SP 68, SP 94 La Quina H18 Krapina: KRD42, KRD44, KRD117	Bayle et al., 2017 Original data
Fossil *H. sapiens* (FHS)	2		Qafzeh 10, 15	Zanolli et al., 2019
Recent humans (RH)	12		Recent humans from China (n=9) Recent humans from Spain (n=3)	Original data

Table 2. 2D enamel thickness variables assessed in TD6 maxillary premolars (in bold) and the comparative sample including extinct and extant specimens/populations.

Sample	**N**	**Tooth class**		**2D AET (mm)**	**2D RET**	**b/a*100 (%)**
ATD6-7	1	UP3		1.02	13.35	70.85
ATD6-13	1			1.00	13.14	70.60
ATD6-69_R	1			1.14	16.82	64.82
ATD6-69_L	1			1.19	16.62	65.52
TD6	**4**		**Mean**	**1.09**	**14.98**	**67.95**
			SD	**0.09**	**2.01**	**3.22**
			Range	**1.00-1.19**	**13.32-16.82**	**64.82-70.85**
EAH	1			1.34	15.11	68.73
SAH	1			1.64	20.62	60.70
AEH	1			1.19	17.53	65.21
NAH	2		Mean	1.24	16.60	66.60
NEA	8		Mean	0.94	13.24	69.38
			SD	0.14	1.57	3.34
			Range	0.66-1.10	10.47-14.83	64.58-74.48
FHS	2		Mean	1.07	16.15	66.32
			SD	0.07	0.31	0.75
			Range	1.02-1.12	15.93-16.37	65.76-66.82
RH	12		Mean	1.08	17.64	63.83
			SD	0.14	1.72	2.59
			Range	0.84-1.27	14.76-19.84	60.15-67.47
		UP4				
ATD6-8	1			1.08	15.44	67.26
ATD6-9	1			1.09	14.82	68.28
ATD6-69_L	1			1.25	18.87	62.95
TD6	**3**		**Mean**	**0.98**	**16.31**	**66.19**
			SD	**0.11**	**2.18**	**2.83**
			Range	**1.03-1.08**	**14.82-18.66**	**62.95-68.28**
EAH	1			1.40	15.97	67.72
AEH	1			1.09	16.65	65.42
NAH	1			1.32	17.91	64.63
EH	1			1.14	17.88	63.22
NEA	6		Mean	1.00	15.17	67.31
			SD	0.16	2.15	3.45
			Range	0.66-1.10	10.47-14.83	64.58-74.48
FHS	2		Mean	1.18	19.21	61.52
			SD	0.10	0.51	0.39
			Range	1.10-1.25	18.83-19.56	61.23-61.78
RH	12		Mean	1.25	20.84	61.25
			SD	0.10	2.38	3.99
			Range	1.07-1.39	16.85-25.06	55.80-70.26

P^{3}: TD6: *H. antecessor* (ATD6-7, ATD6-13, ATD6-69 (2) from Gran Dolina; original data). EAH: East African early *Homo* (specimen KNM-ER 1590 from Koobi Fora, Smith et al., 2012). SAH: South African early *Homo* (specimen SK27 from Swartkrans, Smith et al., 2012). AEH: Asian early *Homo* (Sangiran, Smith et al., 2012). NAH: North African *Homo* (Thomas Quarry 3, Smith et al., 2012. Please note that the Thomas Quarry data does not include individual values, therefore we only employed it for comparative purposes but it was not possible to include it in the boxplots or statistical analyses). NEA: Neanderthals (Wezmeh 1, Zanolli et al., 2019; SP53, SP60 and SP68 from Las Palomas, Bayle et al., 2017; La Quina H18, Krapina D39, D53, D112, original data from Nespos). FHS: fossil *H. sapiens* (Qafzeh 10 and 15, Zanolli et al., 2019). RH: recent humans (original data from Asian and European origin).

P^4: EAH: TD6: *H. antecessor* (ATD6-8, ATD6-8, ATD6-698; original data). East African early *Homo* (specimen KNM-ER 1590 from Koobi Fora, Smith et al., 2012). AEH: Asian early *Homo* (Sangiran, Smith et al., 2012). NAH: North African *Homo* (specimen from Thomas Quarry, Smith et al., 2012). EH: European *Homo* (specimen from Steinheim, Smith et al., 2012). NEA: Neanderthals (specimens SP68 and SP94 from Las Palomas, Bayle et al., 2017; specimens D42, D44 and D117 from Krapina and specimen from La Quina, original data from Nespos). FHS: fossil *H. sapiens* (Qafzeh 10 and 15, Zanolli et al., 2019). RH: recent humans (original data from Asian and European origin).

Table 3. 3D enamel thickness variables assessed in TD6 maxillary premolars (in bold) and the comparative sample including extinct and extant specimens/populations.

Sample	**N**	**Tooth class**		**3D AET (mm)**	**3D RET**	**Vcdp/Vc (%)**
ATD6-7		UP3		1.05	17.46	55.39
ATD6-13				1.02	16.91	56.36
ATD6-69_R				1.26	22.16	50.46
ATD6-69_L				1.28	22.01	50.61
TD6	**4**		**Mean**	**1.15**	**19.63**	**53.21**
			SD	**0.14**	**2.84**	**3.11**
			Range	**1.02-1.28**	**16.91-22.16**	**50.46-56.36**
AEH	1			1.07	17.93	56.48
NEA	8		Mean	1.04	17.96	54.34
			SD	0.18	2.05	2.53
			Range	1.05-1.30	16.60-21.13	50.53-57.72
FHS	2		Mean	1.08	20.14	51.00
			SD	0.08	0.68	0.05
			Range	1.02-1.13	19.65-20.62	50.96-51.03
RH	12		Mean	1.13	22.33	49.70
			SD	0.16	2.93	4.05
			Range	0.93-1.42	18.36-27.90	43.14-56.20
		UP4				
ATD6-8	1			1.09	19.26	52.57
ATD6-9	1			1.07	18.44	54.42
ATD6-69	1			1.35	23.50	49.63
TD6	**3**		**Mean**	**1.17**	**20.40**	**52.21**
			SD	**0.16**	**2.72**	**2.42**
			Range	**1.07-1.35**	**18.44-23.50**	**49.63-54.42**
AEH	1			1.13	19.30	55.06
NEA	6		Mean	1.15	20.96	50.91
			SD	0.19	2.15	2.34
			Range	0.82-1.34	17.87-23.55	47.98-53.54
FHS	2		Mean	1.19	23.32	48.23
			SD	0.06	0.19	0.88
			Range	1.14-1.23	23.18-23.44	47.56-48.81
RH	12		Mean	1.31	26.51	45.18
			SD	0.15	3.72	3.77
			Range	1.08-1.50	20.32-31.78	39.65-52.45

P^3: TD6: *H. antecessor* (ATD6-7, ATD6-13, ATD6-69 (2) from Atapuerca-Gran Dolina; original data). AEH: Asian early *Homo* (specimen PA67 from Zhoukoudian, original data from this study). NEA: Neanderthals (specimen Wezmeh 1, Zanolli et al., 2019; specimens SP53, SP60, SP68 from Las Palomas, Bayle et al., 2017; specimens D39, D53 and D112 from Krapina and specimen H18 from La Quina, original data from Nespos). FHS: fossil *H. sapiens* (Qafzeh 10 and 15, Zanolli et al., 2019). RH: recent humans (original data from Asian and European origin).

P^4: TD6: *H. antecessor* (ATD6-8, ATD6-8, ATD6-69 from Atapuerca-Gran Dolina; original data). AEH: Asian early *Homo* (specimen PA68 from Zhoukoudian, original data from this study). NEA: Neanderthals (specimens SP68 and SP94 from Las Palomas, Bayle et al., 2017; specimens D42, D44 and D117 from Krapina and specimen H18 from La Quina, original data from Nespos). FHS: fossil *H. sapiens* (Qafzeh 10 and 15, Zanolli et al., 2019). RH: recent humans (original data from Asian and European origin).

Table 4. 2D cross-sections thickness variation

Sample	Tooth	LTL	CTL	i	h	CTB	LTB	Bucc	Ling	Occl
TD6	P3	1.54	1.15	1.23	1.07	0.86	1.50	7.63	5.19	11.41
NEA		1.31	0.97	0.90	0.94	0.98	1.33	7.02	6.40	10.41
MH		1.43	1.47	1.13	1.03	0.80	1.32	5.42	3.88	9.83
TD6	P4	1.55	1.22	0.99	1.08	1.03	1.62	6.65	6.04	11.45
NEA		1.39	1.06	1.06	1.07	0.90	1.47	5.76	5.7	11.33
RH		1.61	1.69	1.21	1.33	1.13	1.51	5.32	4.61	12.54

P^3: TD6: *H. antecessor* (ATD6-7, ATD6-13, ATD6-69 (2) from Atapuerca-Gran Dolina; original data). NEA: Neanderthals (specimens D39, D53 and D112 from Krapina and specimen H18 from La Quina, original data from Nespos). RH: recent humans (original data from Asian and European origin). P^4: TD6: *H. antecessor* (ATD6-8, ATD6-8, ATD6-69 from Atapuerca-Gran Dolina; original data). NEA: Neanderthals (specimens D42, D44 and D117 from Krapina and specimen H18 from La Quina, original data from Nespos). RH: recent humans (original data from Asian and European origin).

Figures

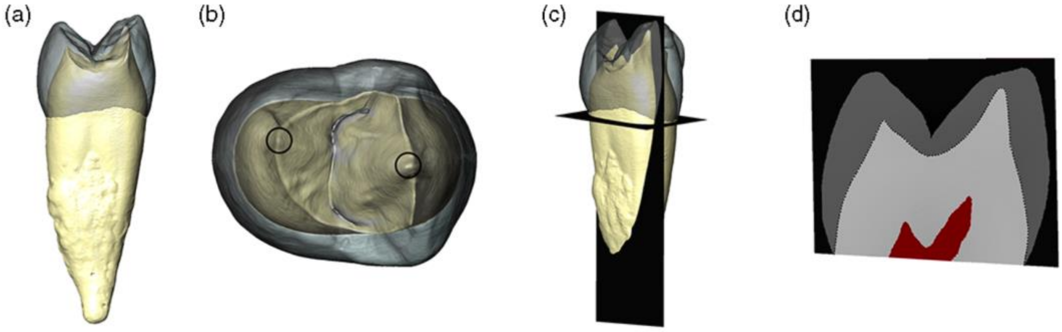

Fig 1. Orientation protocol for enamel thickness measurements in 2D cross sections. A: Buccolingual orientation of the tooth. B: Buccal and lingual horn tips aligned in a horizontal plane. C: Bucco-lingual orientation including both dentine horn tips and the mid-plane between the lowest cervical enamel extension points and maximum bi-cervical diameter. D: In the ideal plane enamel (dark grey) and dentine (light grey) areas, and length of the EDJ (dotted line) are measured (modified from Feeney et al., 2010).

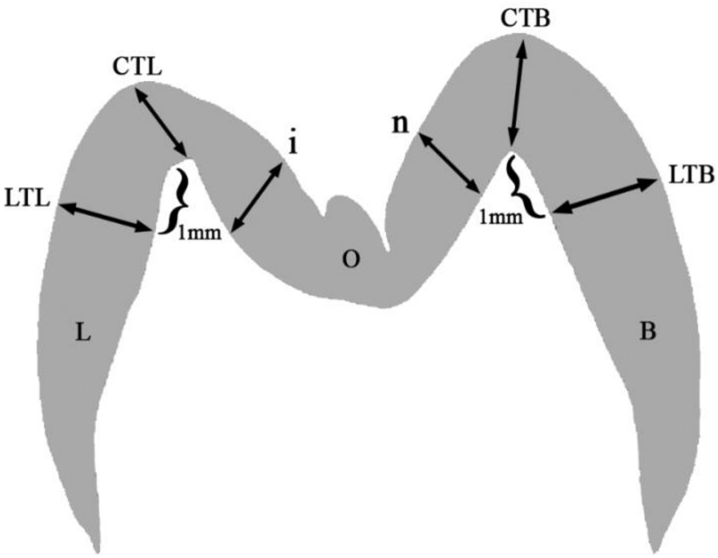

Fig 2. Thickness variability in the 2D cross-sections. Measurements include: LTL: Maximum linear enamel thickness on the lingual side of the lingual cusp, measured perpendicular to the EDJ at a point approximately 1 mm cervical to the dentine horn. CTL: linear enamel thickness on the apex of the lingual cusp, it is the distance between the apex of the dentine horn and the tip of the cusp. i: maximum linear thickness of occlusal enamel on the lingual cusp (protocone), measured perpendicular to the EDJ. h: Maximum linear thickness of occlusal enamel on the buccal cusp (paracone) measured perpendicular to the EDJ. CTB: Linear enamel thickness on the apex of the buccal cusp, it is the distance between the tip of the dentine horn and the tip of the cusp. LTB: Maximum linear enamel thickness on the buccal side of the buccal cusp, measured perpendicular to the EDJ at a point approximately 1 mm cervical to the dentine horn. Using the lingual and buccal linear measurements as markers, buccal (Bucc), lingual (Ling) and occlusal (Occl) areas defined as Bucc: area of the buccal surface from the cervix to the LTC. Ling: area of the lingual surface from the cervix to the CTB. Occl: Area of the occlusal basin between the LTC and the CTB (following Grine, 2005).

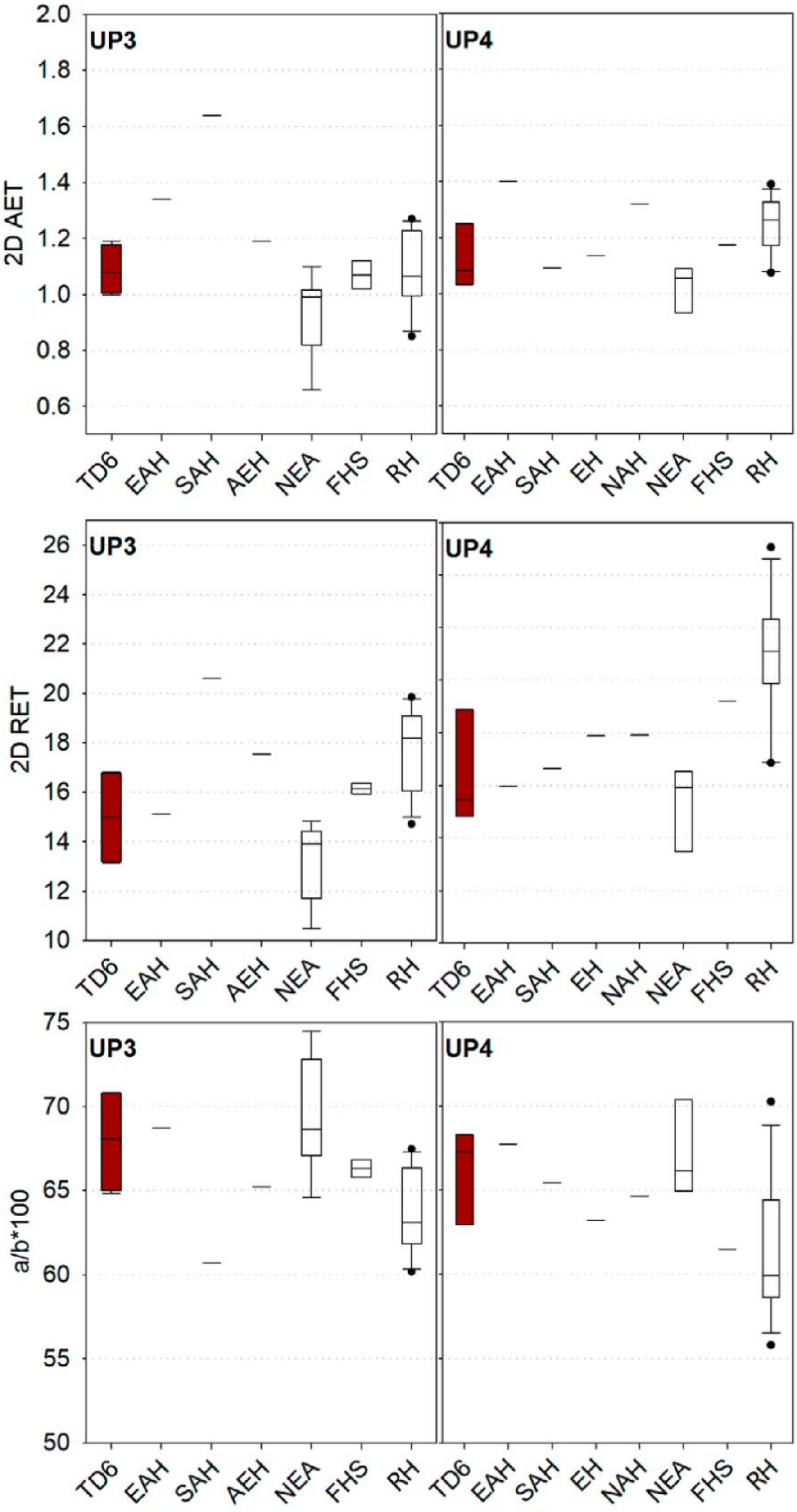

Fig 3. Box Plots depicting 2D values. Values of the average enamel thickness (AET), relative enamel thickness (RET) and percentage of dentine and pulp (a/b*100) in the maxillary premolars of the TD6 and the comparative specimens/samples.

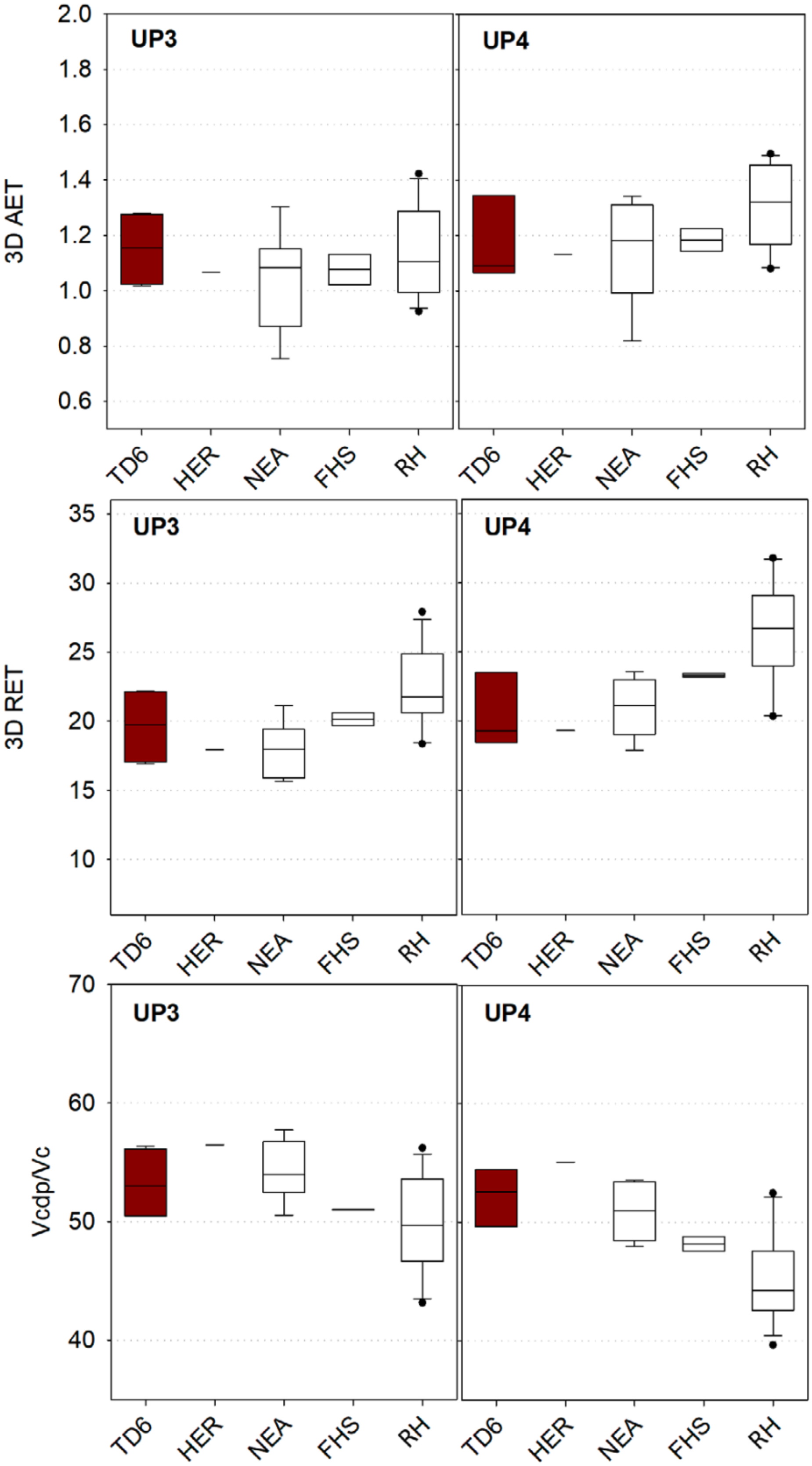

Fig 4. Box Plots depicting 3D values. Values of the average enamel thickness (3D AET), relative enamel thickness (3D RET) and percentage of dentine and pulp (Vcdp/Vc) in the maxillary premolars of the TD6 and the comparative specimens/samples.

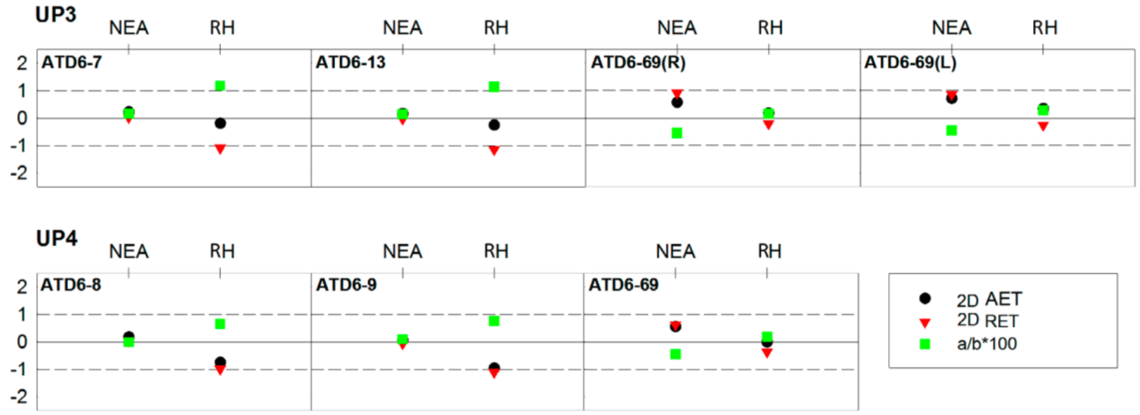

Fig 5. Adjusted Z score of the 2D variables (AET, RET and a/b*100) assessed in the maxillary P^3 (specimens ATD6-7, ATD6-13, ATD6-69 right and left) and P^4 (ATD6-8, ATD6-9 and right ATD6-69) from TD6 and compared to the variation expressed by Neanderthals and recent humans. The solid line passing through zero represents the mean, and the dashed lines correspond to the estimated 95% limit of variation expressed for the two comparative samples (NEA and RH).

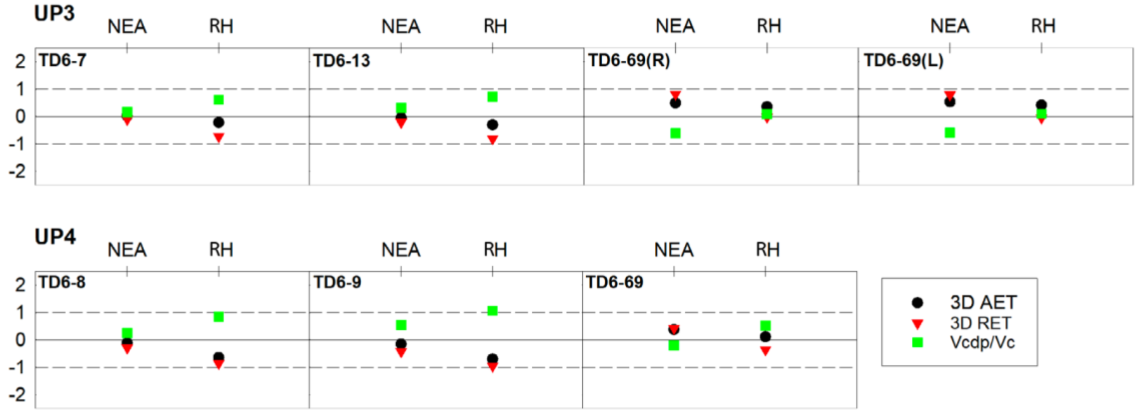

Fig 6. Adjusted Z score of the 3D variables (AET, RET and Vcdp/Vc) assessed in the maxillary P^3 (specimens ATD6-7, ATD6-13, ATD6-69 right and left) and P^4 (ATD6-8, ATD6-9 and right ATD6-69) from TD6 and compared to the variation expressed by Neanderthals and recent humans. The solid line passing through zero represents the mean, and the dashed lines correspond to the estimated 95% limit of variation expressed for the two comparative samples (NEA and RH).

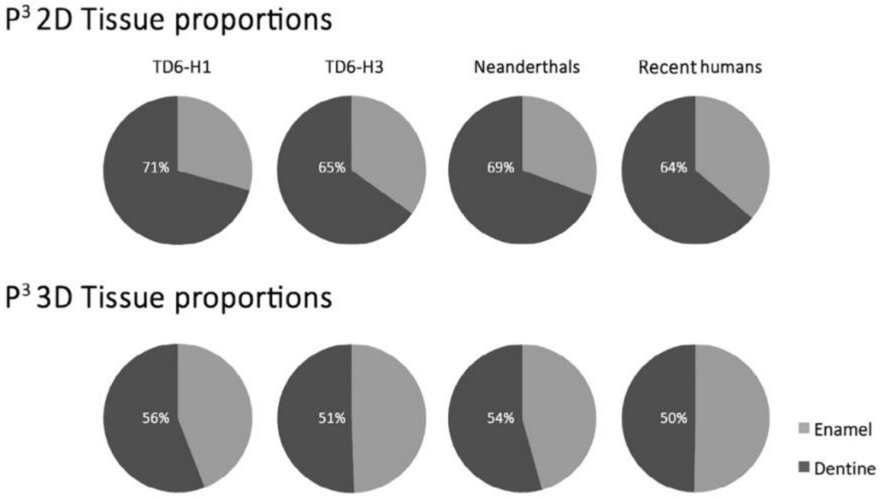

Fig 7. Pie charts showing 2D and 3D relative tissue proportions in TD6 individuals, Neanderthal and recent human P^{3}s. The data show that the difference of dentine proportion is similar across species in 2D and 3D.

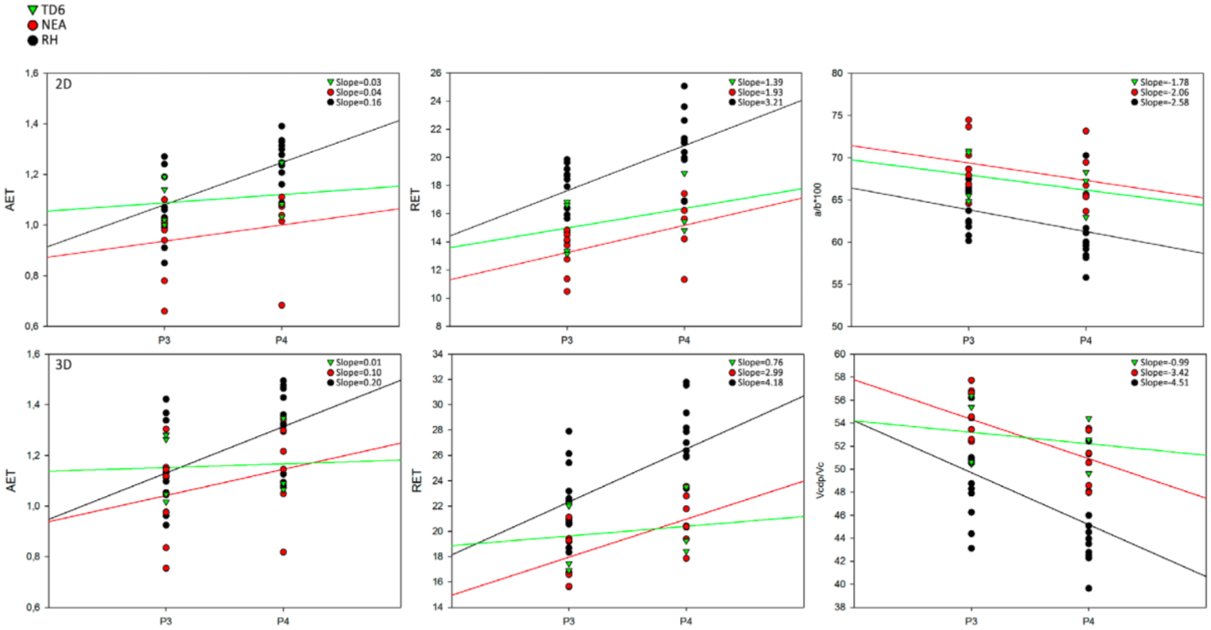

Fig 8. Metameric variation graphs in 2D and 3D variables. The data show that TD6 individuals exhibit the least variation between P^3 and P^4, followed by Neanderthals and recent humans with the greater variation.

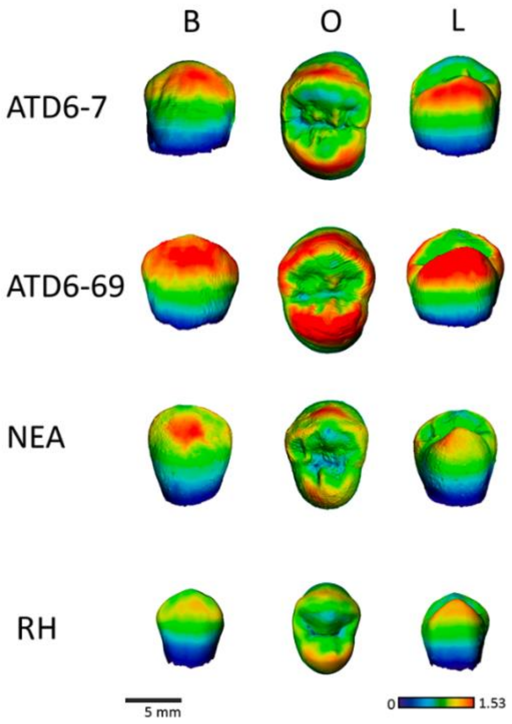

Fig 9. Enamel thickness cartographies of the Atapuerca-TD6 P^3 (ATD6-7 and ATD6-69) compared with those of Neanderthal and recent human. Topographic thickness variation is rendered by a pseudo-colour scale ranging from thinner dark-blue to thicker red. NEA= Neanderthal (La Quina H18) and RH= recent human of Spanish origin (B=buccal, O=occlusal, L=lingual). Scale bar=1.53 for all specimens.

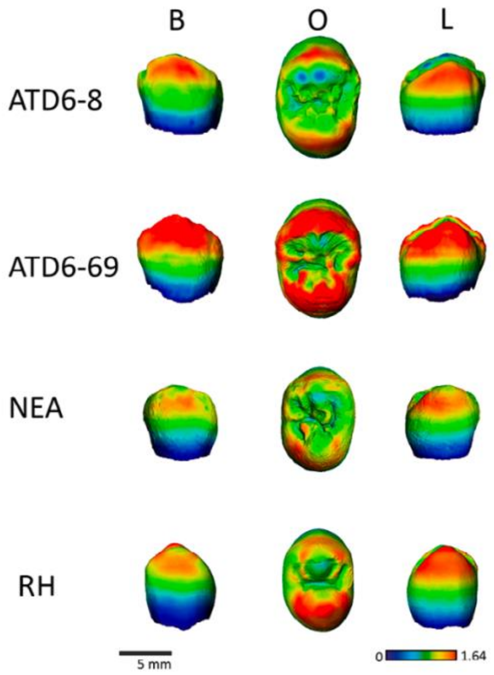

Figure 10. Enamel thickness cartographies of the Atapuerca-TD6 P^4 (ATD6-8 and ATD6-69) compared with those of Neanderthal and recent human. Topographic thickness variation is rendered by a pseudo-color scale ranging from thinner dark-blue to thicker red. NEA= Neanderthal (La Quina H18) and RH= recent human of Spanish origin (B=buccal, O=occlusal, L=lingual). Scale bar=1.64 for all specimens.